

Thermal Effects in Power-Law Fluid Film Lubrication of Rolling/Sliding Line Contact

Gadamsetty Revathi, Venkata Subrahmanyam Sajja, Dhaneshwar Prasad

Abstract: Hydrodynamic lubrication of heavily loaded rigid system of non-symmetric roller bearings is studied to investigate the thermal effects in the operating behavior of line contact under isothermal and adiabatic boundaries. The incompressible power law lubricant is here considered and its consistency is taken to change with hydrodynamic pressure and the corresponding mean lubricant temperature. The flow controlling equations such as momentum, continuity and thermal energy are solved numerically using R-K Fehlberg method. The results obtained particularly, pressure, mean temperature, load and traction profiles are in good agreement with the previous findings.

Index Terms: Hydrodynamic lubrication, Thermal effects, Roller bearings, Non-Newtonian, Power-law, Incompressible.

I. INTRODUCTION

Bearings are used to run the system smoothly. So as to lessen the friction between contacting surfaces, a substance called lubricant can be used between them. The lubricant may be a solid or liquid, and if any load applied normal to the bearing surface may be bolstered by it [1]. The strategy which broadly used to help load and diminish friction is hydrodynamic lubrication. It is likewise realized that the attributes of the bearings, for example, load and speed assume a huge job in the system of lubrication. Subsequently, the traditional hypothesis of hydrodynamic lubrication of highly loaded rigid cylindrical roller bearing problems accentuates to include the viscosity and density to be temperature and pressure contingent [2].

Now-a-days, the effect of temperature in lubrication has gained the attentiveness of investigators. Indeed, the pressure and the temperature of the fluid assume a critical job in collapse of highly loaded line contact problems. Consequently, the impact of temperature produced by the fluid which has heavy pressure due to shearness is no longer imperceptible under the pure rolling and sliding ambience. severe changes of the fluid flow properties due to change of heat are observed [3]. The task of the fluid temperature (T) and hydrodynamic pressure (P) turns out to be much increasingly serious, when the bearing is working at substantial load with more speed [4]. Recently, Dhaneshwar Prasad and Subrahmanyam [2] studied incompressible non-Newtonian lubrication of non-symmetric line contact bearings assuming the power-law consistency to be changed with pressure (P) and the mean temperature (T_m) of the

Revised Manuscript Received on July 05, 2019

Gadamsetty Revathi, Research Scholar, Department of Mathematics, Koneru Lakshmaiah Education Foundation, Guntur-522502, India; and Department of Mathematics, Gokaraju Rangaraju Institute of Engineering and Technology, Hyderabad, India.

Venkata Subrahmanyam Sajja, Department of Mathematics, Koneru Lakshmaiah Education Foundation, Guntur-522502, India

Dhaneshwar Prasad, Department of Mathematics, K M Centre for Post Graduate Studies, Puducherry-605008, India

lubricant under adiabatic and iso-thermal surfaces neglecting inertia effects. Later, Bala subramaniam et al. [5] analyzed the effects of temperature on the friction execution of various lubes in rolling-sliding (line/point) contacting surfaces, and also observed that the boundary friction reduces with gear oils when temperature enhances containing friction reformers while not for other oils. In the greater part of the traditional issues, fluid is considered to be Newtonian. Though, the fluid is liable to have a significant pressure (P) and shear rates, which represent a brief time span, the Newtonian action of the fluid stops to survive [6]. The use of non-Newtonian fluid models in hydrodynamic lubrication containing additives improves and strengthens the life of lubricant; and hence increasing the performance of the bearings [7].

In the modern times, the power-law version has gained the attentiveness of investigators [8]. Hydrodynamic action will be affected by the raise of 'T' in the fluid film because of rapid shear of fluid layer. Such temperature rise may be better approximated for non-Newtonian fluids using power-law model [9]. Prasad et al. [10] studied thermal effects in pure rolling of line contact bearings assuming compressible power-law lubricant under adiabatic condition. Further, Prasad et al. [11] presented the important observations on pressure and mean temperature in case of incompressible power-law lubrication of rolling/sliding problem. Later, Prasad et al. [12] theoretically analyzed the heavily loaded rigid system lubricated by power-law fluids incorporating thermal and inertia effects together with squeezing. Kalin [13] referred to the concept of lubrication by introducing nano particles which is another growing area in today's lubrication science. The main aim of the present work is to explore the performance characteristics of the incompressible power-law lubrication of highly loaded rigid system under isothermal and adiabatic boundaries assuming the variable velocity in the convective part of the energy equation. The consistency of the lubricant is taken to be changed with the pressure (P) and the corresponding mean temperature (T_m); however, surface roughness and compressibility effects have not been included, which is a part of future extension.

II. THEORETICAL MODEL:

2.1 Problem formulation and Governing Equations:

Consider the following momentum and continuity equation under usual assumptions [11] are

$$\frac{dp}{dx} = \frac{\partial}{\partial y} \left[m \left| \frac{\partial u}{\partial y} \right|^{n-1} \frac{\partial u}{\partial y} \right] \quad (1)$$

$$u_x + v_y = 0 \quad (2)$$

where



$$m = m_0 e^{\alpha p - \beta(T_m - T_0)} \quad (3)$$

$$\text{with } T_m = \frac{1}{2h} \int_{-h}^h T dy, \text{ and } h = h_0 + \frac{x^2}{2R} \quad (4)$$

R is the radius of the cylindrical rollers.

2.2 Boundary conditions:

$$u = U_1 \text{ at } y = -h; \text{ and } u = U_2 \text{ at } y = h \quad (5)$$

$$p = 0 \text{ at } x = -\infty; \quad p = 0 \text{ and } \frac{dp}{dx} = 0 \text{ at } x = x_2 \quad (6)$$

where U_1 and U_2 are velocities of the moving surfaces as depicted in Fig.(1).

The fluid velocity gradient conditions are considered as below:

$$\frac{\partial u_1}{\partial y} \geq 0, \delta \leq y \leq h; \quad \frac{\partial u_2}{\partial y} \leq 0, -h \leq y \leq \delta; \quad \text{I:} \quad (7)$$

$$-\infty < x < -x_1$$

$$\frac{\partial u_3}{\partial y} \geq 0, -h \leq y \leq \delta; \quad \frac{\partial u_4}{\partial y} \leq 0, \delta \leq y \leq h; \quad \text{II:} \quad (8)$$

$$-x_1 < x < x_2$$

Solving the equation (1) twice for the zones: $-\infty < x < -x_1$ & $-x_1 < x < x_2$ with the help of the pressure gradients signs (given in Fig.(1)) and the velocity gradient mentioned in (7), one may obtain respectively,

$$u_1 = U_2 + \left(\frac{n}{n+1}\right) \left(\frac{1}{m_1} \frac{dp_1}{dx}\right)^{1/n} \left[(y-\delta)^{\frac{n+1}{n}} - (h-\delta)^{\frac{n+1}{n}} \right], \quad \delta \leq y \leq h$$

$$u_2 = U_1 + \left(\frac{n}{n+1}\right) \left(\frac{1}{m_1} \frac{dp_1}{dx}\right)^{1/n} \left[(\delta-y)^{\frac{n+1}{n}} - (\delta+h)^{\frac{n+1}{n}} \right], \quad -h \leq y \leq \delta \quad (9)$$

$$u_3 = U_1 + \left(\frac{n}{n+1}\right) \left(-\frac{1}{m_2} \frac{dp_2}{dx}\right)^{1/n} \left[(\delta+h)^{\frac{n+1}{n}} - (\delta-y)^{\frac{n+1}{n}} \right], \quad -h \leq y \leq \delta$$

$$u_4 = U_2 + \left(\frac{n}{n+1}\right) \left(-\frac{1}{m_2} \frac{dp_2}{dx}\right)^{1/n} \left[(h-\delta)^{\frac{n+1}{n}} - (y-\delta)^{\frac{n+1}{n}} \right], \quad \delta \leq y \leq h \quad (10)$$

Now, the flux 'Q' in the zone: $-\infty < x < -x_1$, is given by

$$Q = \int_{-h}^h u dy = (U_1 + U_2)h + (U_1 - U_2)\delta$$

$$- \left(\frac{n}{2n+1}\right) \left(\frac{1}{m_1} \frac{dp_1}{dx}\right)^{1/n} \left[(h-\delta)^{\frac{2n+1}{n}} + (h+\delta)^{\frac{2n+1}{n}} \right] \quad (11)$$

$$\text{Now, } Q(-x_1) = (U_1 + U_2)H \quad (12)$$

where the thickness of film H at $x = -x_1$ is considered to be

$$H = 1 + x_1^2 \quad (13)$$

2.3 Reynolds equation:

Then, balancing the flux in (11) and (12), and streamline using dimensionless scheme [14] it can be written as

$$\frac{d\bar{p}_1}{dx} = \bar{m}_1 (\bar{f}_x)^n \quad (14)$$

$$\frac{d\bar{p}_2}{dx} = -\bar{m}_2 (-\bar{f}_x)^n \quad (15)$$

$$(\bar{U} - 1) + E \bar{J}_{13} \bar{f}_x = 0 \quad (16)$$

it is workable only in $-\infty < \bar{x} < -\bar{x}_1$ and $-\bar{x}_1 < \bar{x} < \bar{x}_2$ zones.

$$\text{here } \bar{f}_x = \frac{(\bar{U} + 1)(\bar{h} - \bar{H}) + (\bar{U} - 1)\bar{\delta}}{(\bar{h} + \bar{\delta})^{\frac{2n+1}{n}} + (\bar{h} - \bar{\delta})^{\frac{2n+1}{n}}} \quad \text{and}$$

$$\bar{m}_1 = \bar{m}_0 e^{(\bar{p}_1 - \bar{T}_{m1} + \bar{T}_0)} \text{ etc.}$$

2.4 Equation of Heat Energy:

Consider the following energy equation for the line contact problem under the usual boundary conditions [15]

$$\frac{\rho c}{k} \left(u \frac{dT_m}{dx} \right) = \frac{\partial^2 T}{\partial y^2} + \left(\frac{m}{k} \right) \left| \frac{\partial u}{\partial y} \right| \left(\frac{\partial u}{\partial y} \right)^2 \quad (17)$$

$$\text{The temperature boundary conditions are at } y=h, \frac{\partial T}{\partial y} = 0; \text{ and at } y=-h, T = T_{-h} \quad (18)$$

Now, the fluid film temperatures \bar{T}_{11} and \bar{T}_{12} are computed for the region $-\infty < \bar{x} \leq -\bar{x}_1$ by solving eqn. (4) and given in dimensionless form as:

$$\bar{T}_{11} = \bar{T}_{-h} + A_1 \left\{ \bar{\psi}_{1x} + \frac{\bar{f}_x \bar{g}_{1x}}{n+1} + 2\bar{\gamma} \bar{m}_1 \bar{V}_{1x} (\bar{f}_x)^{n+1} \right\};$$

$$\bar{T}_{12} = \bar{T}_{-h} + A_1 \left\{ \bar{\psi}_{2x} + \frac{\bar{f}_x \bar{g}_{2x}}{n+1} + 2\bar{\gamma} \bar{m}_1 \bar{V}_{2x} (\bar{f}_x)^{n+1} \right\} \quad (19)$$

Similarly, one can get for the region $-\bar{x}_1 < \bar{x} < \bar{x}_2$,

$$\bar{T}_{21} = \bar{T}_{-h} + A_2 \left\{ \bar{\psi}_{2x} + \frac{\bar{f}_x \bar{g}_{2x}}{n+1} + 2\bar{\gamma} \bar{m}_2 \bar{V}_{2x} (-\bar{f}_x)^{n+1} \right\};$$

$$\bar{T}_{22} = \bar{T}_{-h} + A_2 \left\{ \bar{\psi}_{1x} + \frac{\bar{f}_x \bar{g}_{1x}}{n+1} + 2\bar{\gamma} \bar{m}_2 \bar{V}_{1x} (-\bar{f}_x)^{n+1} \right\} \quad (20)$$

Finally, the mean temperature \bar{T}_{m1} and \bar{T}_{m2} may be obtained as:

$$\bar{T}_{m1} - \bar{T}_{-h} - \bar{P}_e \frac{d\bar{T}_{m1}}{dx} \left[\bar{H}_x + \bar{g}_x \bar{f}_x \right] - 2\bar{\gamma} \bar{m}_1 \bar{V}_x (\bar{f}_x)^{n+1} = 0, \quad -\infty < \bar{x} \leq -\bar{x}_1 \quad (21)$$

$$\bar{T}_{m2} - \bar{T}_{-h} - \bar{P}_e \frac{d\bar{T}_{m2}}{dx} \left[\bar{H}_x + \bar{g}_x \bar{f}_x \right] - 2\bar{\gamma} \bar{m}_2 \bar{V}_x (-\bar{f}_x)^{n+1} = 0, \quad -\bar{x}_1 < \bar{x} < \bar{x}_2 \quad (22)$$

2.5 Load (W) and Traction forces (T_F):

The load carrying components W is calculated in the direction of y-axis is given by $W = \int_{-\infty}^{x_2} p dx$ (23)

The non-dimensional load (\bar{W}) is given by

$$\bar{W} = \int_{-\infty}^{\bar{x}_2} \bar{p} d\bar{x} \quad (24)$$

The traction forces T_f at both the surfaces are obtained by integrating the shear stress τ for the entire length and one may get



$$T_{Fh-} = - \int_{-\infty}^{x_2} \tau_{y=-h} dx ; \text{ and } T_{Fh+} = - \int_{-\infty}^{x_2} \tau_{y=h} dx \quad (25)$$

Dimensionless tractions are

$$\bar{T}_{Fh-} \left(= \alpha \frac{T_{F_0}}{h_0} \right) = - \int_{-\infty}^{\bar{x}_2} \bar{\tau}_{\bar{y}=\bar{h}} d\bar{x} ; \text{ and}$$

$$\bar{T}_{Fh+} = - \int_{-\infty}^{\bar{x}_2} \bar{\tau}_{\bar{y}=\bar{h}} d\bar{x} \quad (26)$$

III. RESULTS AND DISCUSSION:

In order to perform the numerical computations, the following values are used in this problem:

$$U_2 = 400 \text{ cm/s} , h_0 = 4 \times 10^{-4} \text{ cm} , \alpha = 1.6 \times 10^{-9} \text{ dyne}^{-1} \text{ cm}^2 , R=3 \text{ cm} , \bar{\gamma} = 1000.5 , \bar{T}_{-h} = 1.4 .$$

Here $\bar{P}_e \rightarrow 0$ corresponds to the case without convection.

3.1 Pressure (\bar{p}) profile:

The pressure distribution \bar{p} trends are presented in Fig. (2) and Fig. (3). It is seen from Fig. (2) that \bar{p} increases with power-law index 'n', and this kind of the behavior was observed by [2, 16]. Further, Fig. (3) shows that the lubricant pressure \bar{p} almost increases everywhere as \bar{U} increases for some value of n. This is similar to the results of Prasad et al. [17].

3.2 Mean Temperature (\bar{T}_m) profile:

\bar{T}_m is elaborated through Figs. (4-6), for different values of 'n', \bar{U} and \bar{P}_e . \bar{T}_m enhances with 'n' indicates that \bar{T}_m for dilatants fluid is more when compared with pseudo plastic and Newtonian fluids [10, 11]. Further, it is clear from Fig. (5) that \bar{T}_m enhances with \bar{U} for some fixed entities of 'n' and \bar{P}_e . This implies that the sliding temperature is greater than that of pure rolling [18].

3.3 Consistency (\bar{m}) Profile:

The lubricant consistency \bar{m} is depicted in Fig. (7) for various values of 'n' and the increase in consistency with 'n' can be observed for $\bar{U}=1.2$. The similar kind of graph was presented by Prasad et al. [12]. It can be confirmed mathematically that the increase or decrease of consistency is the increase or decrease in the resultant of \bar{p} and \bar{T}_m .

3.4 $\bar{\delta}$ - profile:

The rough sketch of $\bar{\delta}$ -profile is given in Fig. (1). An alike profile is given by Prasad et al. [11]. The qualitative manner of $\bar{\delta}$ with numerical calculations for n=1.15, $\bar{U}=1.2$ and $\bar{P}_e=0.4$ are presented in Fig. (8).

3.5 Load and Traction:

The estimated dimensionless load \bar{W} , the traction forces at both lower and upper surfaces are given in Figs. (9-11) respectively. Fig.(9) shows the increasing trend of \bar{W} with 'n' and \bar{U} , it is in conformity with the previously published results [10].

The traction forces \bar{T}_{Fh+} and \bar{T}_{Fh-} have been determined for two surfaces for different values of 'n' and \bar{U} . \bar{T}_{Fh+} and \bar{T}_{Fh-} rises with 'n' and \bar{U} . The trends of the traction forces are similar to [16] comparatively with 'n' and \bar{U} . Further, it is identified that both the traction forces converge to the unique value as $\bar{U} \rightarrow 1$. This physically shows the symmetricity of rollers.

3.6 Velocity profile:

Lubricant velocity profiles \bar{u} verses \bar{y} at different locations of the lubricant in the place between the surfaces are computed and presented in Figs. (12-14) respectively for the regions before, after, and also at the point where the maximum pressure ($-\bar{x}_1$) occurs. The first two figures have the same characteristics i.e. parabolas with vertices downward and upward in the regions before and after $-\bar{x}_1$. But, the velocity profile seems to be linear at $-\bar{x}_1$. The vertices below the x-axis as depicted in Fig. (12) (i.e. at $\bar{x}=-4,-3,-2$) show some back flows near the inlet. Reverse flow was also shown by Dong Zhu and Wen [19]. As the fluid progresses, the back flow is over. The same is also shown roughly in Fig. (1). It is clear from Fig. (14) that the velocity of the lubricant decreases linearly as \bar{y} increases at $-\bar{x}_1$.

IV. CONCLUSION:

The problem is attempted to investigate the thermal lubrication analysis of rolling /sliding line contact bearings lubricated with an incompressible power-law lubricant under the assumption of isothermal and adiabatic boundaries. The pressure and the thermal equations with convection, conduction and dissipation both are solved for \bar{p} and \bar{T}_m simultaneously for various values of \bar{U} (sliding parameter) and 'n' (power law index). The facts given below are drawn from the results of this work.

- (i) A notable increase in \bar{p} and hence the load is observed with increase of 'n' and \bar{U} , presented in Figs. (2-3).
- (ii) A remarkable increase in \bar{T}_m is observed with increase of 'n' and \bar{U} . It is also important to note down that the variations in the mean temperature, presented in Figs. (4-6) have remarkable impact of 'n'.
- (iii) The traction force \bar{T}_{Fh+} for the upper surface increases from 1.0 to 1.1 as \bar{U} increases, and then decreases up to 1.5 as \bar{U} increases. Further, the traction force \bar{T}_{Fh-} for the lower surface decreases as \bar{U} increases but not significantly.

REFERENCES:

- Manojlović, J., "Dynamics of SAMs in Boundary Lubrication", 2013, Tribology in Industry, Vol. 35, No.3, pp. 200-207.
- Venkata Subrahmanyam Sajja and Dhaneshwar Prasad, "Characterization of Lubrication of Asymmetric Rollers including Thermal Effects", Industrial Lubrication and Tribology, 2015, Vol. 67, No. 3, pp. 246-255.
- Popov, V. L., and Psakhie, S. G., "Numerical Simulation Methods in Tribology", 2007, Tribology International, Vol. 40, pp. 916-923.
- Wang J., Shiyue Qu, and Peiran Yang, "Simplified Multigrid Technique for the Numerical Solution to the Steady-State and Transient EHL Line Contacts and the Arbitrary Entrapment EHL Point Contacts", 2001, Tribology International, Vol. 34, pp. 191-202.
- Balasubramaniam Vengudusamy, Alexander Grafl, Franz Novotny-Farkas, and Werner Schofmann, "Influence of Temperature on the friction performance of gear oils in rolling-sliding and pure sliding contacts", 2014, Lubrication Science, Vol. 26, pp. 229-249.
- Hirst, W., and Moore, A.J., "EHD Lubrication of High Pressure", 1978, Proc. Roy. Soc. Lond., Vol. A 360, PP. 403-425.
- Ertugrul Durak, Ozlem Salmon, and Cahit Kurbanoglu, "Analysis of Effect of Oil Additive into Friction Coefficient Variations on Journal Bearing using Artificial Network", 2008, Industrial Lubrication and Tribology, Vol. 60(6), pp. 309-316.
- Sinha P., Singh C., "Lubrication of Cylinder on a Plane with a non-Newtonian Fluid Considering Cavitation", 1982, Journal of Lubrication Technology, Vol. 104, pp. 168-172.
- Mishra P. C., "Analysis of a Rough Elliptic Bore Journal Bearing using Expectancy Model of Roughness Characterization", 2014, Tribology in Industry, Vol. 36(2), pp. 211-219.
- Prasad D., Singh P., Sinha P., "Non-Uniform Temperature in Non-Newtonian Compressible Fluid Film Lubrication of Rollers", 1988, Journal of Tribology, Vol. 110, pp. 653-658.
- Prasad D., Shukla J.B., Singh P., Sinha P., and Chhabra R.P., "Thermal Effects in Lubrication of Asymmetrical Rollers", 1991, Tribology International, Vol. 24, pp. 239-246.
- Prasad D., Singh P., and Prawal Sinha, "Thermal and Inertia Effects in Hydrodynamic Lubrication of Rollers by a Power Law Fluid Considering Cavitation", 1993, Journal of Tribology, Vol. 115, pp. 319-326.
- Kalin, M., "Traditional problems, yet new challenges in lubrication science", 2013, Lubrication Science, Vol. 25, pp. 249-250.
- Prasad, D., Subrahmanyam, S.V., Panda, S.S., "Thermal Effects in Hydrodynamic Lubrication of Asymmetric Rollers using Runge-Kutta Fehlburg Method", 2012, International Journal of Engineering Science and Advanced Technology, Vol. 2, pp. 422-437.
- Tsann-Rong Lin, "Thermal EHD Lubrication of Rolling/Sliding Contacts with a Power-Law Fluid", 1992, Wear, Vol.54, pp. 77-93.
- Dhaneshwar Prasad and Venkata Subrahmanyam Sajja, "Non-Newtonian Lubrication of Asymmetric Rollers with thermal and inertia effects", Tribology Transactions, 2016, Vol. 59, No. 5, pp. 818-830.
- Prasad, D., Singh, P., and Sinha, P., "Thermal and Squeezing Effects in Non-Newtonian Fluid Film Lubrication of Rollers", 1987, Wear, Vol. 119, pp. 175-190.
- Sadeghi, F. and Dow, T.A., "Thermal Effects in Rolling/Sliding Contacts – Part 2: Analysis of Thermal Effects in Fluid Films", 1987, Journal of Tribology, Vol. 109, pp. 512-518.
- Dong Zhu, and Wen, S.Z., "A Full Numerical Solution for The Thermal Elastohydrodynamic Problem in Elliptical Contacts, 1984, ASME Journal of Tribology, Vol. 106, pp. 246-254.

6. APPENDIX:

$$\bar{A}_1 : \bar{p}_e \frac{dT_{m1}}{dx}$$

$$\bar{A}_2 : \bar{p}_e \frac{dT_{m2}}{dx}$$

$$B : n^2 / [2\bar{h}(3n+1)(4n+1)]$$

$$E : (2n+1)/(n+1)$$

$$E_5 : 2n/(3n+1)$$

$$\bar{g}_x : [nB\bar{J}_{1x} - \bar{J}_{2x} - n\bar{J}_{3x} + \bar{J}_{4x}]/(n+1)$$

$$\bar{g}_{1x} :$$

$$(n/2)E_5\bar{J}_{5x} + [(2n+1)/2]\bar{h}^2(\bar{h} + \bar{\delta})^{\frac{n+1}{n}} + (\bar{\psi}_{5x})(\bar{\psi}_{3x}) - \bar{\psi}_{6x}$$

$$\bar{g}_{2x} :$$

$$(n/2)E_5\bar{J}_{6x} + [(2n+1)/2](\bar{h}^2 - \bar{y}^2)(\bar{h} + \bar{\delta})^{\frac{n+1}{n}} + (\bar{\psi}_{5x})(\bar{\psi}_{4x}) - \bar{\psi}_{6x}$$

H : Lubricant film thickness

\bar{h}_1 : Film thickness at $x = -x_1$

\bar{h}_0 : Minimum film thickness

\bar{h} : \bar{h} / \bar{h}_0 etc.

$$\bar{H} : (1/12\bar{h})[(\bar{U} + 1)\bar{h}^3 + (\bar{U} - 1)\bar{\delta}^3] - \bar{h}^2\left(\frac{\bar{U}}{2} + 1\right)$$

$$\bar{J}_{1x} : (\bar{h} - \bar{\delta})^{\frac{4n+1}{n}} + (\bar{h} + \bar{\delta})^{\frac{4n+1}{n}}$$

$$\bar{J}_{2x} :$$

$$[(2n+1)/12\bar{h}]\left[(\bar{h}^3 - \bar{\delta}^3)(\bar{h} - \bar{\delta})^{\frac{n+1}{n}} + (\bar{h}^3 + \bar{\delta}^3)(\bar{h} + \bar{\delta})^{\frac{n+1}{n}}\right]$$

$$\bar{J}_{3x} : (E_5/2)(\bar{h} + \bar{\delta})^{\frac{3n+1}{n}} + \bar{h}(\bar{h} - \bar{\delta})^{\frac{2n+1}{n}}$$

$$\bar{J}_{4x} : [(2n+1)/2]\bar{h}^2\left[2(\bar{h} - \bar{\delta})^{\frac{n+1}{n}} + (\bar{h} + \bar{\delta})^{\frac{n+1}{n}}\right]$$

$$\bar{J}_{5x} : (\bar{y} - \bar{\delta})^{\frac{3n+1}{n}} - (\bar{h} + \bar{\delta})^{\frac{3n+1}{n}}$$

$$\bar{J}_{6x} : (\bar{\delta} - \bar{y})^{\frac{3n+1}{n}} - (\bar{h} + \bar{\delta})^{\frac{3n+1}{n}}$$

$$\bar{J}_{11} : (\bar{y} - \bar{\delta})^{\frac{n+1}{n}} - (\bar{h} - \bar{\delta})^{\frac{n+1}{n}}$$

$$\bar{J}_{12} : (\bar{\delta} - \bar{y})^{\frac{n+1}{n}} - (\bar{h} + \bar{\delta})^{\frac{n+1}{n}}$$

$$\bar{J}_{13} : (\bar{h} - \bar{\delta})^{\frac{n+1}{n}} - (\bar{h} + \bar{\delta})^{\frac{n+1}{n}}$$

m: Lubricant consistency

m_0 : Consistency at ambient pressure and temperature

\bar{m} : $2 m c_n \alpha$ etc.

$$\bar{m}_1 : \bar{m}_0 e^{(\bar{p}_1 - \bar{T}_{m1} + \bar{T}_0)}$$

n: Power-law index

\bar{p} : Hydrodynamic pressure

\bar{p} : αp etc.

Q : Lubricant volume flux

R : Radius of the cylinder

T : Temperature of the lubricant

T_m : Mean film temperature

T_0 : Ambient temperature

\bar{T} : βT etc.

T_{Fh} : Traction force etc.

\bar{T}_{Fh} : Non-Dimensional traction force ($-2\alpha T_{Fh} / h_0$) etc.

U_1, U_2 : Velocities of the lower and upper surfaces

u, v : Velocity components in x and y direction

- \bar{u} : u / U_1 etc.
- \bar{V}_x : $\bar{J}_{3x} - B\bar{J}_{1x}$
- \bar{V}_{1x} : $(\bar{y} + \bar{h})(\bar{h} - \bar{\delta})^{\frac{2n+1}{n}} - (E_5 \bar{J}_{5x} / 2)$
- \bar{V}_{2x} : $(\bar{y} + \bar{h})(\bar{h} - \bar{\delta})^{\frac{2n+1}{n}} - (E_5 \bar{J}_{6x} / 2)$
- W: Load in y-direction
- \bar{W} : Non-dimensional load ($= \alpha W / (Rh_0)^{1/2}$)
- x,y : Co-ordinate axes
- \bar{x} : Dimensionless distance in x-direction
 ($= x / \sqrt{2Rh_0}$)
- x_1 : Point of maximum pressure
- x_2 : Point of cavitation
- α : Coefficient of pressure
- β : Coefficient of temperature
- δ : Location of points where velocity gradient is zero
- $\bar{\delta}$: δ / h_0
- $\bar{\gamma}$: $\left(\frac{U_2 h_0 \beta}{2k\alpha} \right) \sqrt{\frac{h_0}{2R}}$
- \bar{p}_e : $\frac{\rho c U_2 h_0}{k} \sqrt{\frac{h_0}{2R}}$
- ϕ : $\frac{\rho c u_m}{k} \left(\frac{dT_m}{dx} \right)$ etc.
- $\bar{\psi}_{1x}$: $\frac{\bar{y}^2}{2} - \bar{y}\bar{h} - \bar{h}^2 \left(\frac{\bar{U}}{2} + 1 \right)$
- $\bar{\psi}_{2x}$: $\frac{\bar{y}^2 \bar{U}}{2} - \bar{y}\bar{h} - \bar{h}^2 \left(\frac{\bar{U}}{2} + 1 \right)$
- $\bar{\psi}_{3x}$: $\bar{y}\bar{h} - (\bar{y}^2 / 2) + \bar{h}^2$
- $\bar{\psi}_{4x}$: $\bar{y}\bar{h} + \bar{h}^2$
- $\bar{\psi}_{5x}$: $(2n+1)(\bar{h} - \bar{\delta})^{\frac{n+1}{n}}$
- $\bar{\psi}_{6x}$: $n(\bar{y} + \bar{h})(\bar{h} - \bar{\delta})^{\frac{2n+1}{n}}$

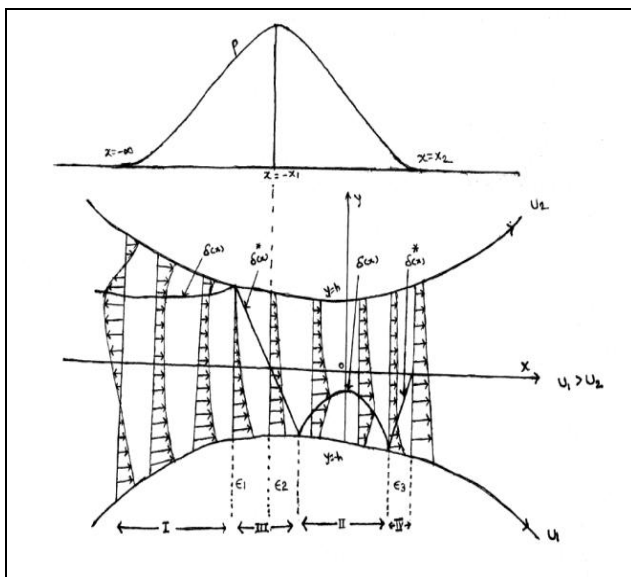


Fig. (1): Lubrication of asymmetric rollers

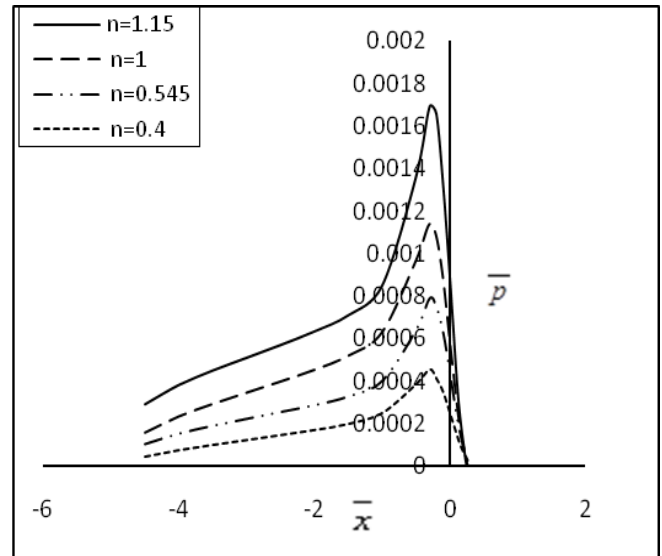


Fig. (2): \bar{P} profile for $\bar{v}=1.2$

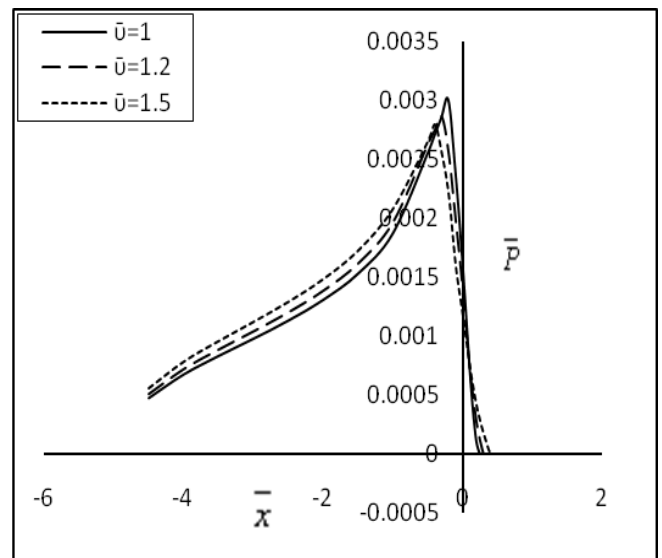


Fig. (3): \bar{P} profile for $n=1.15$

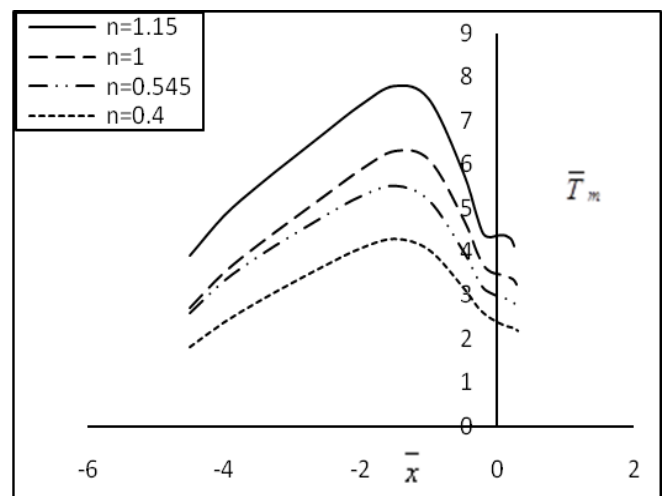


Fig.(4): \bar{T}_m profile for $\bar{v}=1.2$

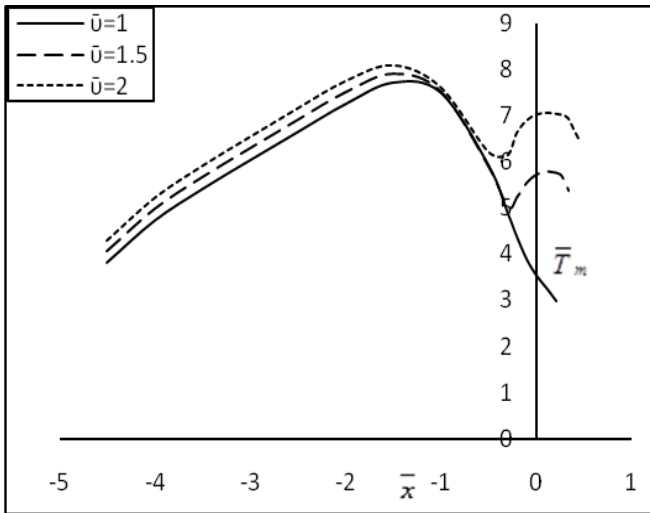


Fig.(5): \bar{T}_m profile for $n=1.15$

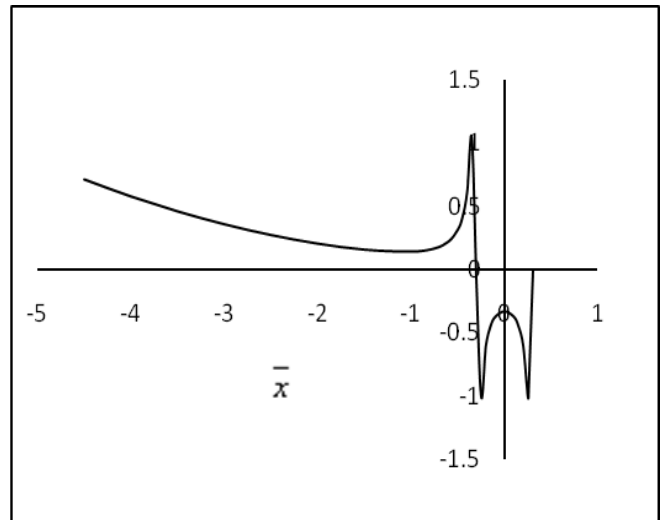


Fig. (8): $\bar{\delta}$ - Profile for $\bar{v}=1.2$

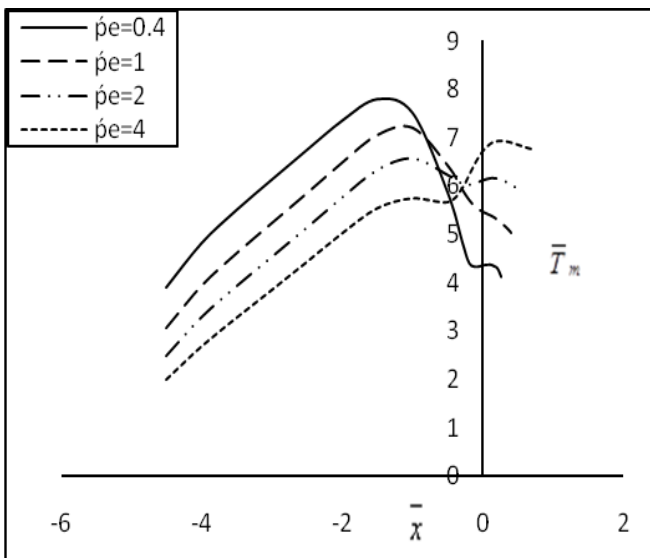


Fig.(6): \bar{T}_m profile for $\bar{v}=1.2, n=1.15$

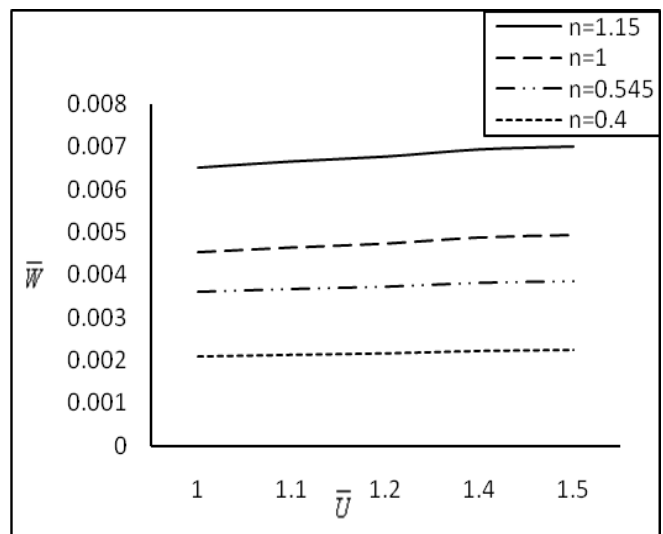


Fig. (9): Load \bar{W} versus \bar{v}

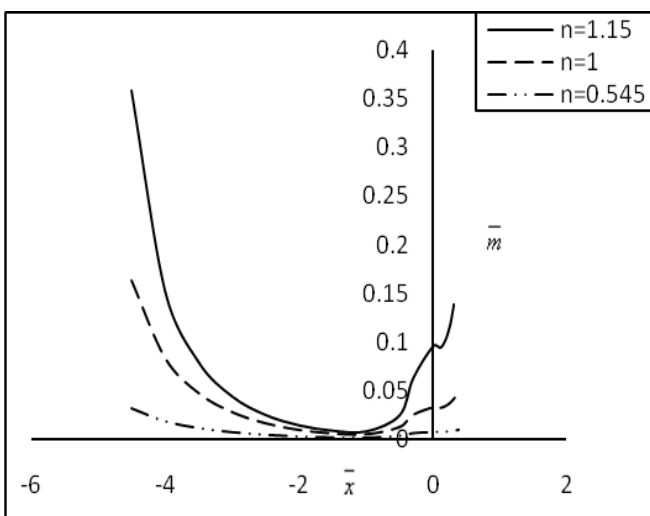


Fig.(7): Consistency \bar{m} for $\bar{v}=1.2$

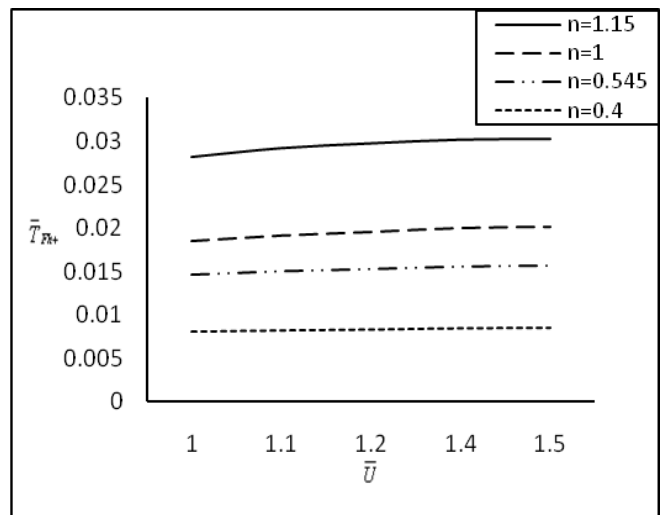


Fig. (10): Traction \bar{T}_{Fh+} versus \bar{v}

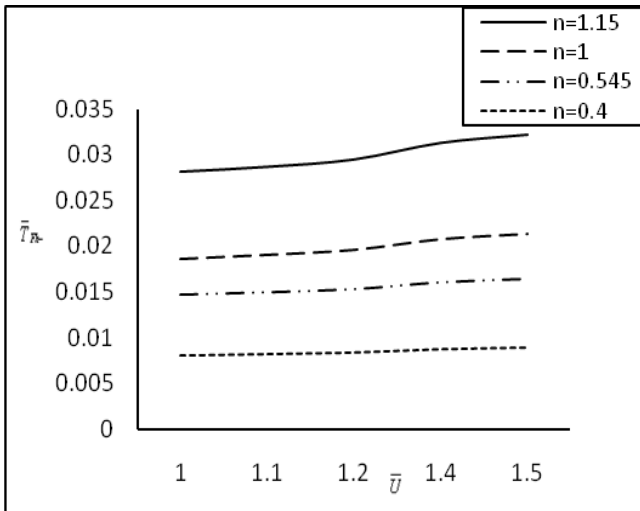


Fig. (11): Traction \bar{T}_{FH} versus \bar{u}

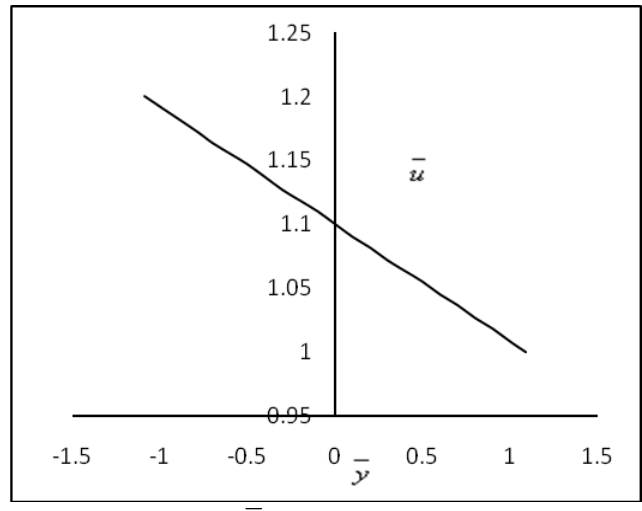


Fig. (14): Velocity \bar{u} at point of maximum pressure

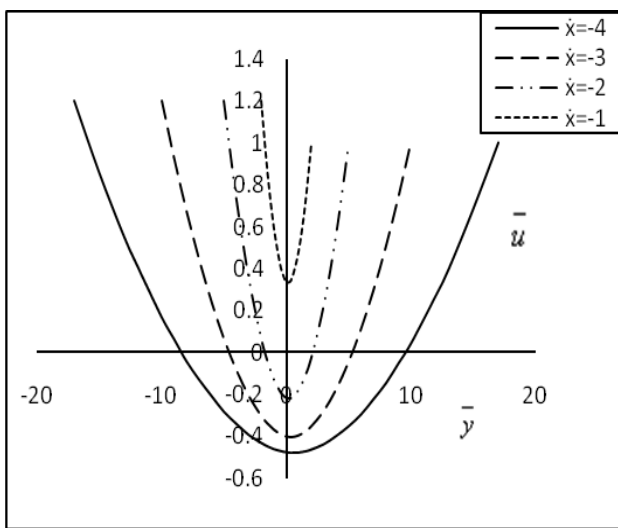


Fig. (12): Velocity \bar{u} profile

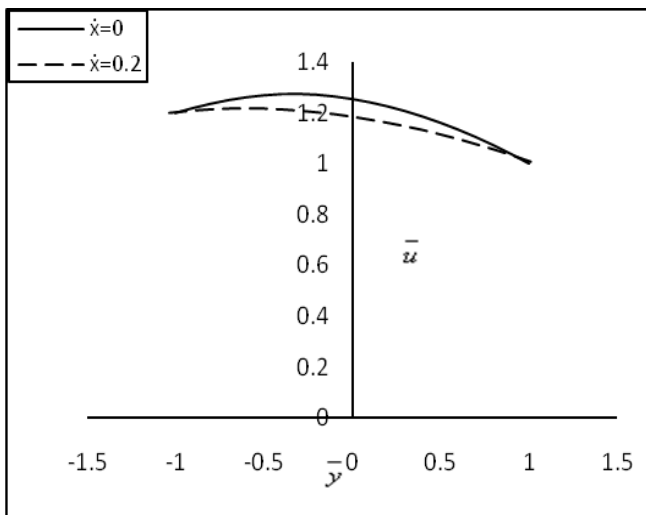


Fig. (13): Velocity \bar{u} profile

AUTHORS PROFILE



G. Revathi is an Asst. Professor of Mathematics in Gokaraju Rangaraju Institute of Engineering and Technology, Hyderabad, India. She obtained M. Sc. degree from Acharya Nagarjuna University, Guntur. She is pursuing Ph.D. from Koneru Lakshmaiah Education Foundation, Guntur, India. She has 10 years of teaching experience.



Dr. Venkata Subrahmanyam Sajja, is an Associate Professor of Mathematics in Koneru Lakshmaiah Education Foundation, Guntur, India. He obtained his Ph. D. degree in Fluid Dynamics in 2016 from Dravidian University, Kuppam, Andhra Pradesh, India. He has a good number of research publications in various National and International Journals. His research interest is Hydrodynamic theory of lubrication of bearings.



Dr. Dhaneshwar Prasad, is an Associate Professor and HOD of Mathematics in Kanchi Mamunivar Centre for Post Graduate Studies, Puducherry, India. He received his Doctoral degree from IIT, Kanpur. He served 28 years in teaching and 22 years research. His area of interest is Fluid Dynamics. He has a good number of research publications in various National and International journals.